1-9-2004

AKT/Protein Kinase B Regulation of BCL Family Members during Oxysterol-induced Apoptosis

Antonio E. Rusiñol
Quillen-Dishner College of Medicine, rusinol@etsu.edu

Douglas Thewke
Quillen-Dishner College of Medicine, thewke@etsu.edu

June Liu
Quillen-Dishner College of Medicine

Natalie Freeman
Quillen-Dishner College of Medicine

Sankhavaram R. Panini
Quillen-Dishner College of Medicine

See next page for additional authors

Follow this and additional works at: https://dc.etsu.edu/etsu-works

Citation Information

AKT/Protein Kinase B Regulation of BCL Family Members during Oxysterol-induced Apoptosis

Creator(s)

Antonio E. Rusiñol, Douglas Thewke, June Liu, Natalie Freeman, Sankhavaram R. Panini, and Michael S. Sinensky

AKT/Protein Kinase B Regulation of BCL Family Members during Oxysterol-induced Apoptosis*

Antonio E. Rusiñol‡, Douglas Thewke‡, June Liu, Natalie Freeman, Sankhavaram R. Panini, and Michael S. Sinensky§

From the Department of Biochemistry and Molecular Biology, James H. Quillen College of Medicine, East Tennessee State University, Johnson City, Tennessee 37614-0581

Cells of the vasculature, including macrophages, smooth muscle cells, and endothelial cells, exhibit apoptosis in culture upon treatment with oxidized low density lipoprotein, as do vascular cells of atherosclerotic plaque. Several lines of evidence support the hypothesis that the apoptotic component of oxidized low density lipoprotein is one or more oxysterols, which have been shown to induce apoptosis through the mitochondrial pathway. Activation of the mitochondrial pathway of apoptosis is regulated by members of the BCL family of proteins. In this study, we demonstrate that, in the murine macrophage-like cell line P388D1, oxysterols (25-hydroxycholesterol and 7-ketocholesterol) induced the degradation of the prosurvival protein kinase AKT (protein kinase B). This led, in turn, to the activation of the BCL-2 homology-3 domain-only proteins BIM and BAD and down-regulation of the anti-apoptotic multi-BCL homology domain protein BCL-x_L. These responses would be expected to activate the pro-apoptotic multi-BCL homology domain proteins BAX and BAK, leading to the previously reported release of cytochrome *c* observed during oxysterol-induced apoptosis. Somewhat surprisingly, small interfering RNA knockdown of BAX resulted in a complete block of the induction of apoptosis by 25-hydroxycholesterol.

Many of the pathological events associated with the development of atherosclerosis are believed (1) to be mediated by oxidized low density lipoprotein (ox-LDL).[1] The constitutive uptake by macrophages of ox-LDL is through specialized scavenger receptors, resulting in these cells becoming lipid-laden foam cells (2). The formation of such cells is the hallmark of atherosclerosis. Furthermore, ox-LDL has been shown to be cytotoxic to macrophages (3) through a process requiring such receptors (4, 5). This cytotoxicity could be very important in the atherogenicity of ox-LDL through the lysis of foam cells and the concomitant deposition of lipids in the coronary vasculature.

The cytotoxic effects of ox-LDL have been shown to proceed, at least in part, through apoptotic pathways, in general (reviewed in Refs. 6 and 7), as well as in macrophages, in particular (3, 8, 9).

The cholesterol oxidation products (oxysterols) found in ox-LDL (10) have been recognized as a probable basis for its cytotoxicity (11, 12), at least in part, via apoptotic mechanisms (7, 13, 14). A model compound for such oxysterols is 25-hydroxycholesterol (25-OHC), which has been shown to induce apoptosis in monocyte-macrophage (9, 15, 16) and lymphoid (17, 18) cell lines in the range of 1–10 μM. Prior studies have been consistent with the activation of the mitochondrial death pathway by oxysterols with its canonical cytochrome *c* release (19, 20). Cytochrome *c* release from mitochondria is regulated, in turn, through the activation of pro-apoptotic BCL family members, along with possible inactivation of anti-apoptotic BCL family members (21). In this study, we describe the role of the AKT-regulated BAX/BAD pathway in oxysterol-induced apoptosis of murine macrophage cell lines.

EXPERIMENTAL PROCEDURES

Materials—RAW 264.7 cells were purchased from American Type Culture Collection (Manassas, VA). P388D1 cells (MAB variant) were provided by Dr. Edward Dennis (University of California, San Diego, CA) (22). RPMI 1640 medium and Dulbecco's modified Eagle's medium were from Invitrogen. NovaCell I fetal bovine serum was from Nova-Tech (Grand Island, NE). All other cell culture reagents were obtained from Invitrogen. 5,8,11,14-Eicosatetraynoic acid (ETYA), Ac-DEVD-aldehyde, Ac-DEVD-7-amino-4-trifluoromethyl coumarin, and arachidonyl trifluoromethyl ketone (AACOCF$_3$) were purchased from BIOMOL Research Labs Inc. (Plymouth Meeting, PA). Oxysterols were purchased from STERALOIDS, Inc. (Wilton, NH). All antibodies were purchased from Cell Signaling Technology, Inc. (Beverly, MA), with the exception of anti-AKT1/2 antibody (Santa Cruz Biotechnology, Santa Cruz, CA), anti-Myc antibody (Upstate Biotechnology, Inc., Charlottesville, VA), and anti-HSP70 antibody (Stressgen Biotech Corp., Victoria, British Columbia, Canada). Peroxidase-conjugated secondary antibodies were from Pierce. pEGFP-C3 was from Clontech. Proteasome inhibitor I was from Calbiochem. MitoTracker™ Red was from Molecular Probes, Inc. (Eugene, OR).

Cell Culture—All cell lines were maintained in a humidified atmosphere of 5% CO$_2$ and 95% air at 37 °C. RAW 264.7 cells were cultured in RPMI 1640 medium supplemented with 10% fetal bovine serum, 10 mM Hepes buffer (pH 7.4), 2 mM glutamine, 1 mM sodium pyruvate, 100 units/ml penicillin, 100 μg/ml streptomycin, and 50 μM 2-mercaptoethanol. P388D1 cells were cultured in Dulbecco's modified Eagle's medium supplemented with 10% fetal bovine serum, 2 mM glutamine, 1 mM sodium pyruvate, 100 units/ml penicillin, and 100 μg/ml streptomycin.

Caspase-3 Assay—P388D1 cells were seeded at 2×10^6/well in 12-well culture plates, and RAW 264.7 cells at 2.5×10^6/well in 6-well culture plates. The medium was supplemented with 25-OHC dissolved in ethanol or an equivalent volume of ethanol alone (control treatments). Inhibitor (ETYA or AACOCF$_3$) was added to the medium 2 h prior to the addition of 25-OHC. Following an 18-h incubation, the adherent and non-adherent cells were collected by scraping and centrifugation at $1000 \times g$ for 5 min. The cells were washed with ice-cold

[1] The abbreviations used are: ox-LDL, oxidized low density lipoprotein; 25-OHC, 25-hydroxycholesterol; ETYA, 5,8,11,14-eicosatetraynoic acid; AACOCF$_3$, arachidonyl trifluoromethyl ketone; GFP, green fluorescent protein; myr, myristoylated; BH3, BCL-2 homology-3; STAT, signal transducer and activator of transcription.

phosphate-buffered saline, resuspended in lysis buffer A (10 mM Tris (pH 7.5), 130 mM NaCl, 1% Triton X-100, 10 mM sodium P_i, and 10 mM sodium PP_i), incubated on ice for 10 min, and centrifuged at 12,000 × *g* for 20 min at 4 °C. The supernatant or extract was assayed for protein using the micro-BCA kit (Pierce) and for caspase-3 activity as follows. Equivalent amounts of each sample were incubated for 2.5 h at 37 °C in
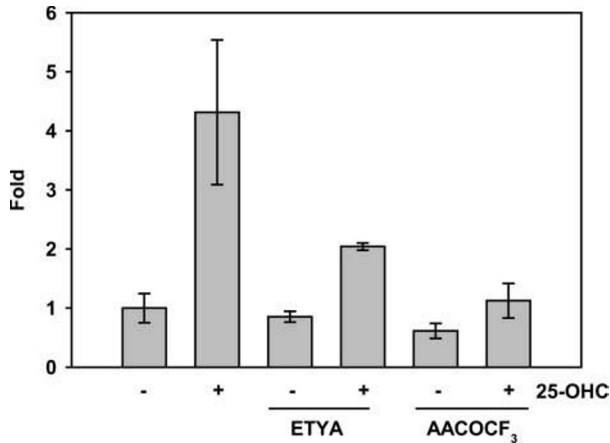

FIG. 1. **A specific inhibitor of cytosolic phospholipase A₂ (AACOCF₃) and a general inhibitor of arachidonate metabolism (ETYA) prevent induction of caspase-3 by 25-OHC in P388D1 cells.** P388D1 cells were cultured in medium with or without 20 μM AACOCF₃ or 10 μM ETYA for 2 h prior to the addition of 25-OHC or vehicle (ethanol). Following an 18-h incubation, the cells were harvested, and caspase-3 and "caspase-3-like" activities were measured as described under "Experimental Procedures." The results are expressed as -fold increases in fluorescence relative to the mean fluorescence determined for control treatments (vehicle only). The data represent the mean ± S.D. of triplicate treatments.

caspase assay buffer (20 mM Hepes (pH 7.5), 10% glycerol, and 2 mM dithiothreitol) containing 5 μM caspase-3 substrate (Ac-DEVD-7-amino-4-trifluoromethyl coumarin) in the presence and absence of a caspase-3-specific inhibitor (Ac-DEVD-aldehyde) added at 100 nM 30 min prior to the addition of the substrate. Liberated 7-amino-4-trifluoromethyl coumarin was measured using a spectrofluorometer (FluroMax 3 equipped with a microplate reader, Jobin-Yvon Inc.) with an excitation wavelength of 400 nm and an emission wavelength of 505 nm. For each sample, the net caspase-3 activity was determined by subtracting the relative fluorescent light units obtained in the presence of the inhibitor from the relative fluorescent light units obtained in the absence of the inhibitor and normalizing to the protein content of the sample. Each treatment was performed in triplicate, and the data are presented as the mean ± S.D.

BAD-GFP Fusion Protein—The *Bad* open reading frame was excised from pEBG-mBAD (Cell Signaling Technology, Inc.) with HindIII and NotI and ligated in-frame into pEGFP-C3 after the creation of an appropriate NotI site using the QuikChange kit (Stratagene). The finished construct was confirmed by sequencing and transfected into RAW 264.7 cells using GeneJammer (Stratagene).

Detection of BAD-GFP in RAW 264.7 Cells—Transiently transfected RAW 264.7 cells were incubated overnight on glass chambered coverslips. Cells were then washed and incubated with 25-OHC (10 μg/ml) for 6 h. After washing with phosphate-buffered saline, cells were observed live under a fluorescence microscope. In colocalization experiments, mitochondria were also stained with MitoTracker™ Red following the manufacturer's instructions. Confocal images were obtained by digital deconvolution of 10-slice stacks acquired on a Nikon Diaphot 200 equipped with a Photometrics Sensys cooled CCD digital camera or Nikon D100 Oncor Z-drive and Oncor Image software.

Bax Gene Suppression—*Bax* gene suppression was achieved by stably transfecting cells with pSi-*Bax*, a plasmid that generates small interfering RNAs that target *Bax* mRNA for degradation. To produce pSi-*Bax*, the following complementary oligonucleotides were annealed and cloned into ApaI/EcoRI-digested pSilencer (Ambion Inc., Austin, TX): *Bax* 1, ACTGGTGCTCAGGCCCTGTTCAAGAGACAGGGCCTTGAGCACCAGTTTTTTT; and *Bax* 2, AATTAAAAAAACTGGTGCTC-

FIG. 2. **25-OHC induces proteasome-dependent AKT degradation.** *A*, P388D1 cells were treated with 10 μg/ml 25-OHC for 12 h, and AKT kinase activity was measured as described under "Experimental Procedures" using glycogen synthase kinase-3β fusion protein as substrate. The data represent the mean ± S.D. of triplicate measurements. *B*, P388D1 cells were treated with 10 μg/ml 25-OHC for different times, and the levels of total AKT were measured by immunoblotting as described under "Experimental Procedures." *C*, P388D1 cells were pulse-labeled with 100 μCi/ml Tran³⁵S-label and chased in the absence (○) or presence (●) of 10 μg/ml 25-OHC as described under "Experimental Procedures." At different times, total AKT was immunoprecipitated, and radioactivity was measured by SDS-PAGE and phosphorimaging. The extrapolated half-lives for AKT were ∼8 h and ∼100 min in the control and 25-OHC-treated cells, respectively. *D*, total AKT levels were determined by immunoblotting after treatment with 10 μg/ml 25-OHC for 12 h in the presence or absence of 15 μM proteasome inhibitor I (*PI-I*).
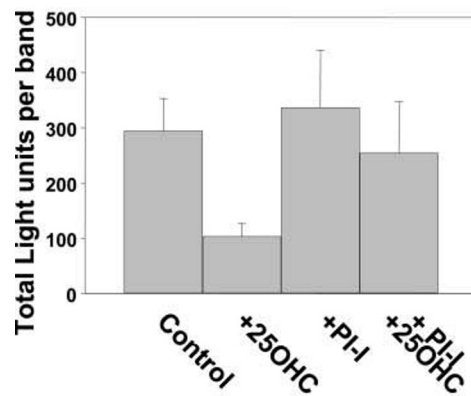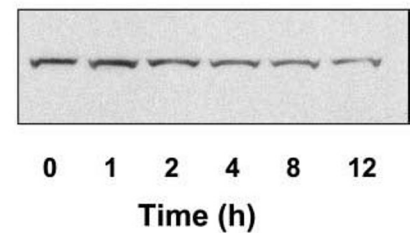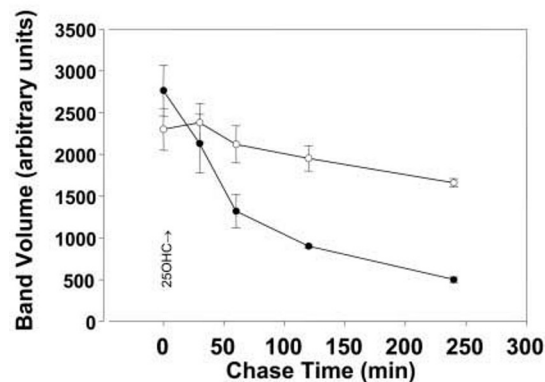
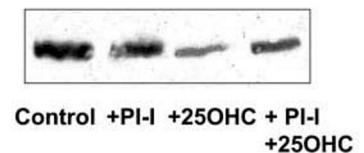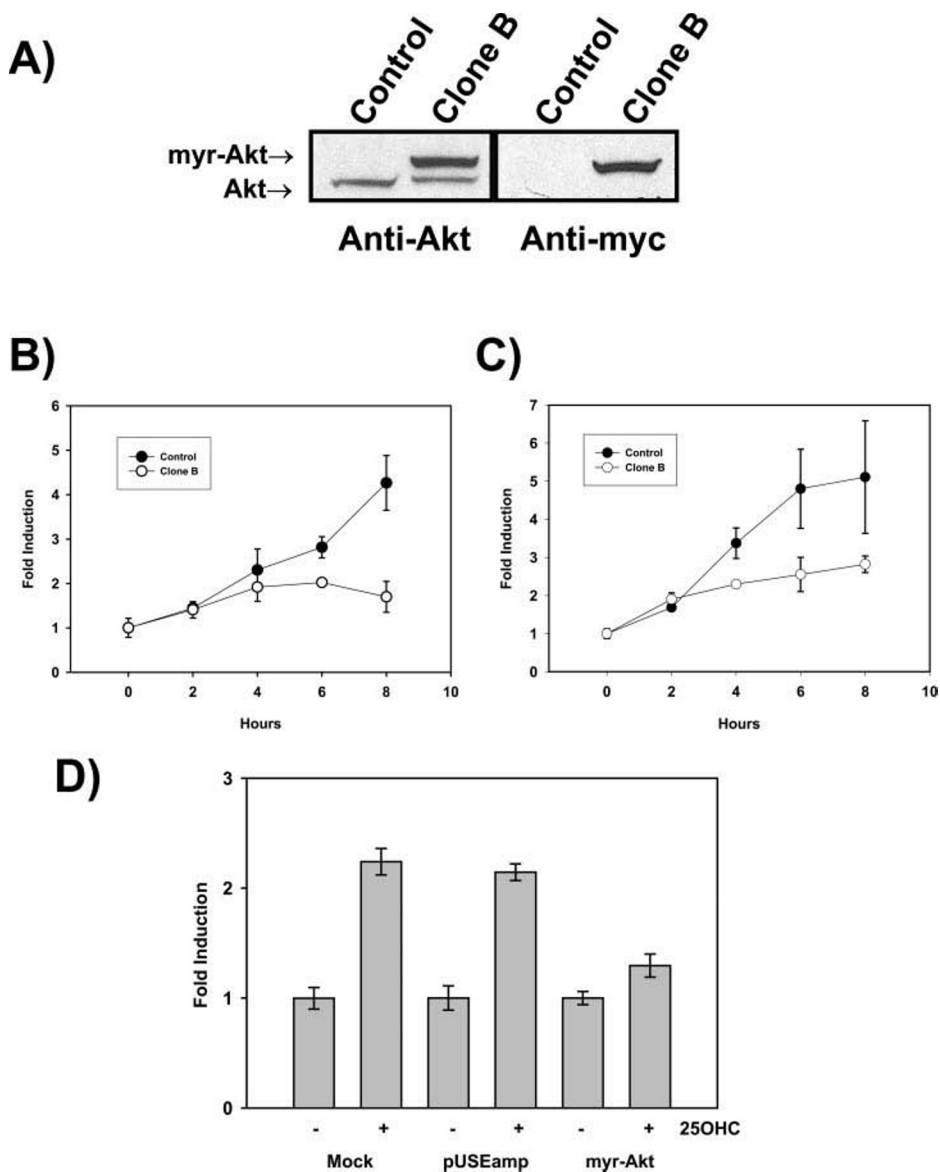FIG. 3. **Ectopic expression of constitutively active AKT reduces 25-OHC induction of caspase-3 activity in P388D1 cells.** *A*, whole cell lysates obtained from P388D1 cells stably transfected with a myr-*Akt* expression vector (clone B) or the empty vector (control) were subjected to SDS-PAGE, transferred to polyvinylidene difluoride membranes, and immunoblotted using anti-total AKT and anti-Myc antibodies as indicated. *B* and *C*, clone B (○) and control (●) cells were incubated with medium containing either 10 μg/ml 25-OHC or 10 μg/ml 7-ketocholesterol, respectively, for various times. The medium was then replaced with medium without oxysterol, and incubation was continued for 16 h. The -fold induction of caspase-3 activity was determined as described for Fig. 1. *D*, P388D1 cells transiently transfected with no DNA (*Mock*), empty vector (pUSEamp), or vector containing *Akt* cDNA (myr-*Akt*) were incubated in medium with or without 10 μg/ml 25-OHC for 6 h as indicated. The medium was refreshed without oxysterol supplementation; and following a 16-h incubation, the -fold induction of caspase-3 activity was determined.

AAGGCCCTGTCTCTTGAACAGGGCCTTGAGCACCAGTGGCC. The negative control vector pSi-Random*Bax* was constructed by ligating the following annealed, custom-synthesized oligonucleotides of randomized *Bax* target sequence into ApaI/EcoRI-digested pSilencer: Random*Bax* 1, ACCGCTCGAGCGTGCTAGTTTCAAGAGAACTAGCACGCTCGAGCGGTTTTTTT; and Random*Bax* 2, AATTAAAAAAACCGCTCGAGCGTGCTAGTTCTCTGAAACTAGCACGCTCGAGCGGTGGCC.

P388D1 cells (1×10^6) were cotransfected with a plasmid carrying the neomycin gene, pEGFP (Clontech), and either pSi-*Bax* or pSi-Random*Bax* using LipofectAMINE Plus (Invitrogen) according to the manufacturer's directions. Stable clones were first selected by infinite dilution in medium containing 1 mg/ml G418 for 7 days, followed by 14 days in 0.25 mg/ml G418. G418-resistant clones were screened by PCR for integration of the pSilencer vector. The PCR positive G418-resistant clones were then subjected to selection in medium containing 10 μg/ml 25-OHC for 68 h. The surviving cells were expanded and maintained in medium containing 500 μg/ml G418. No 25-OHC-resistant clones were obtained from PCR positive G418-resistant pRandom*Bax* clones. The suppression of BAX expression was determined by immunoblotting whole cell lysates prepared from the isolated clones, wild-type cells, and G418-resistant pRandom*Bax* clones using anti-BAX antibody.

Expression of Constitutively Active AKT—P388D1 cells were stably transfected with a vector expressing Myc-His-tagged mouse AKT1 (activated) under the control of the cytomegalovirus promoter (Upstate Biotechnology, Inc.) using LipofectAMINE Plus according to the manufacturer's directions. Stable clones were isolated by selection in medium containing 1 mg/ml G418 for 6 days, followed by 10 days in 250 μg/ml G418. The G418-resistant clones were isolated, expanded, and

screened for expression of the Myc-AKT fusion protein by immunoblotting with anti-total AKT1/2 antibody (Cell Signaling Technology, Inc.) and anti-Myc antibody. Positive Myc-AKT clones were maintained in medium containing 250 μg/ml G418.

For transient transfection experiments, P388D1 cells were seeded at 2×10^6/well in 6-well tissue culture plates. Twenty-four hours later, the cells were rinsed with phosphate-buffered saline, refed standard growth medium, and transfected with pUSEamp or with pUSEamp containing myristoylated (myr) *Akt* cDNA using Tojene™ transfection reagent (Avanti Polar Lipids, Inc.) according to the manufacturer's directions. Following transfection, expression of the transfected construct was allowed to proceed for 24 h prior to the addition of oxysterol and analysis of caspase-3 activity.

Cell Lysis and Immunoblotting—P388D1 cells were grown to a density of 2×10^6/ml in regular growth medium supplemented with either vehicle (ethanol) or increasing amounts of 25-OHC. After different periods of time, cells were spun and treated with lysis buffer B (20 mM Tris (pH 7.5), 150 mM NaCl, 1 mM EDTA, 1 mM EGTA, 1% Triton X-100, 2.5 mM sodium pyrophosphate, 1 mM β-glycerol phosphate, 1 mM Na_3VO_4, and 1 μg/ml leupeptin) and incubated on ice for 30 min. Insoluble debris was removed from the extracts by centrifugation for 10 min at 10,000 × g, and the protein concentration in the supernatants was determined by micro-BCA assay. Proteins were resolved by SDS-PAGE on 4–12% NuPAGE gels (Invitrogen) and transferred to polyvinylidene difluoride membranes (Immobilon-P, Millipore Corp.). The membranes were stained with SYPRO®Ruby protein stain (Molecular Probes, Inc.) to ascertain equivalent loading of the gel and efficient transfer of proteins to the membranes before immunoblotting. The blots
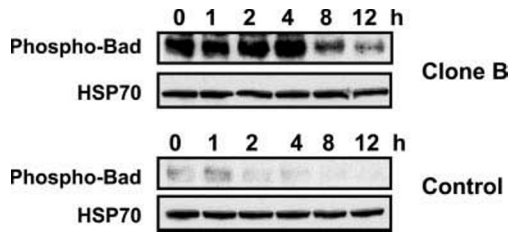
FIG. 4. **Effect of 25-OHC on phosphorylation of BAD.** Equal amounts of whole cell lysates from AKT-expressing clone B and control P388D1 cells cultured in medium supplemented with 10 μg/ml 25-OHC for various time periods were subjected to immunoblotting using anti-phospho-Ser-136 BAD antibody as described under "Experimental Procedures." The membranes were then stripped and immunoblotted with anti-HSP70 antibody to control for equivalent loading of the gel and efficient transfer of proteins to the membrane.

were then processed using antibodies specific for the protein of interest and the appropriate peroxidase-conjugated secondary antibodies following manufacturers' directions. The proteins of interest were visualized by enhanced chemiluminescence using SuperSignal® West Pico chemiluminescent substrate (Pierce) as directed.

Pulse-Chase Experiments—P388D1 cells were grown in methionine-deficient medium for 2 h and then pulsed with Tran^{35}S-label (100 μCi/ml; ICN) for 3 h. Cells were then washed and chased for different time periods in regular growth medium containing 1 mM unlabeled methionine and either vehicle (ethanol) or 10 μg/ml 25-OHC. Cells were lysed as described above and subjected to immunoprecipitation with anti-AKT antibodies. Assays were performed using Seize™-coated plate immunoprecipitation kits (Pierce) according to the manufacturer's instructions. After binding, washing, and elution, the presence of radiolabeled AKT in the precipitates was examined by SDS-PAGE and phosphorimaging.

AKT Kinase Assay—The active form of AKT was measured using a nonradioactive AKT kinase assay kit (Cell Signaling Technology, Inc.) following the manufacturer's instructions. Essentially, an antibody to AKT was used to selectively immunoprecipitate AKT from cell lysates. The immunoprecipitate was then incubated with glycogen synthase kinase-3β fusion protein in the presence of ATP and kinase buffer, allowing immunoprecipitated AKT to phosphorylate glycogen synthase kinase-3β. Phosphorylation of glycogen synthase kinase-3β was then measured by immunoblotting using anti-phospho-Ser-21/9 glycogen synthase kinase-3α/β antibody and quantitated by phosphorimaging.

RESULTS

25-OHC Induces Apoptosis in P388D1 Cells through a Process Dependent on Arachidonate Metabolism—We have previously characterized oxysterol induction of apoptosis in both a fibroblast cell line (CHO-K1) and a monocyte-macrophage cell line (THP-1) as being dependent on arachidonate release and metabolism (9). Because of difficulties we encountered in transfection of THP-1 cells and the well established use of the murine macrophage P388D1 cells in studies of arachidonate metabolism (22), we determined whether P388D1 cells undergo apoptosis in response to oxysterols in a similar fashion. We confirmed a prior report (16) that 25-OHC induces apoptosis in P388D1 cells and also demonstrated, as was observed for the other cell lines, that the induction of apoptosis was blocked both by the cytosolic phospholipase A$_2$ inhibitor AACOCF$_3$ and by ETYA, an inhibitor of arachidonate metabolism (Fig. 1).

25-OHC Down-regulates AKT in P388D1 Cells—AKT (protein kinase B) has been well characterized as an anti-apoptotic kinase (24) that transduces cellular survival signals in many cell types (25). In particular, a critical role for AKT has been ascribed to the survival of macrophages (26). We therefore examined the effect of overnight treatment with 25-OHC on the activity of AKT in the murine macrophage cell line P388D1. Activity was assayed with glycogen synthase kinase-3β as substrate. The results clearly indicate that AKT activity was down-regulated in P388D1 cells in response to treatment with 25-OHC (Fig. 2*A*).

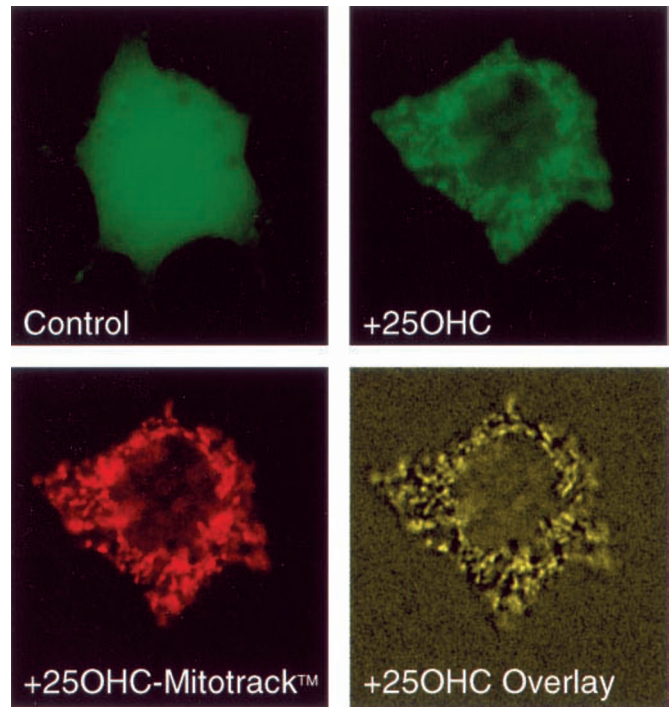The mechanism of down-regulation of AKT was explored by

FIG. 5. **25-OHC induces BAD translocation to the mitochondria.** RAW 264.7 cells were transiently transfected with BAD-GFP fusion protein. After 16 h, cells were treated with 10 μg/ml 25-OHC and incubated for 6 h. The localization of the BAD-GFP chimera was determined by fluorescence microscopy as described under "Experimental Procedures." The same cell is shown before and after treatment. Mito-Tracker is a fluorescent probe that specifically stains mitochondria.
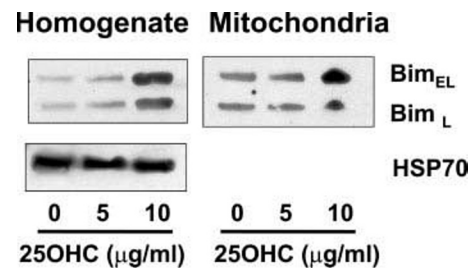

FIG. 6. **25-OHC treatment increases total and mitochondrial BIM levels.** P388D1 cells were treated with 10 μg/ml 25-OHC for 12 h, and the mitochondrial and total cellular levels of BIM were measured by immunoblotting. Polyvinylidene difluoride membranes were then stripped and reprobed with anti-HSP70 antibody as a control for loading and transfer.

immunoblot and radioimmunoprecipitation experiments. Immunoblot analysis demonstrated that oxysterol treatment produced a reduction in the level of total AKT in P388D1 cells (Fig. 2*B*). Pulse-chase radioimmunoprecipitation studies revealed that 25-OHC treatment greatly enhanced the rate of degradation of AKT (Fig. 2*C*). Furthermore, the effect was observed with no time lag after 25-OHC addition, suggesting that this is an early signaling event. We also examined the effect of treatment with proteasome inhibitor I on the cellular levels and activity of AKT in 25-OHC-treated cells. This was done to determine whether this enhanced degradation rate was responsible for the decrease in its activity as well as to gain insight into the mechanism of regulated degradation. The results demonstrate that inhibition of the degradation of AKT significantly attenuated the loss of its activity in response to 25-OHC treatment (Fig. 2, *A* and *D*). Therefore, the primary mechanism by which 25-OHC down-regulates the activity of AKT appears to be through stimulation of its rate of degradation. This mecha-
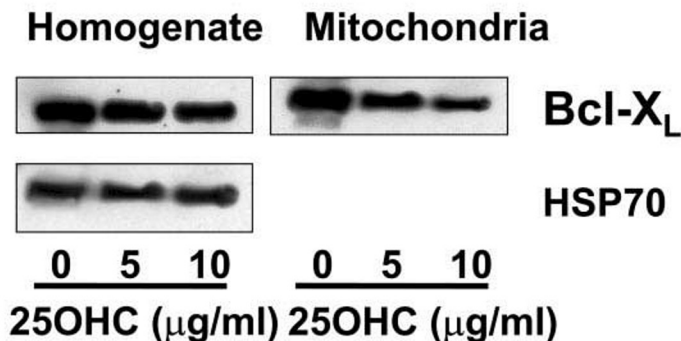
A)

FIG. 7. **Suppression of BAX expression protects P388D1 cells from 25-OHC-induced apoptosis.** *A*, P388D1 cells were treated with different amounts of 25-OHC for 12 h, and the mitochondrial and total cellular levels of BCL-x$_L$ were measured by immunoblotting. Polyvinylidene difluoride membranes were subsequently stripped and reprobed for HSP70 as a control for loading and transfer. *B*, shown are the results from immunoblot analysis of BAX and BAK protein levels in whole cell lysates from P388D1 cells stably transfected with pSi-*Bax*, an small interfering RNA expression vector targeting *Bax* mRNA (*Si-Bax #1*), or pSi-Random*Bax*, a control vector expressing randomized *Bax* target sequence (*R-Bax*). *C*, the pSi-*Bax* (●) and pRandom*Bax* (○) clones were cultured for 16 h in medium containing increasing amounts of 25-OHC as indicated. Control cells received an equal amount of vehicle only (ethanol). Caspase-3 activity was then determined as described for Fig. 1. Each treatment was done in triplicate, and the data are presented as the mean ± S.D.

B)
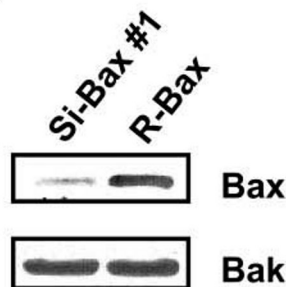
C)
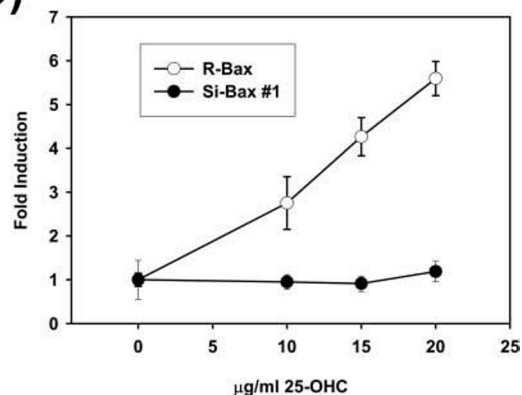
nism of degradation is also consistent with an early regulated event.

We wanted to confirm this putative critical role for AKT signaling in 25-OHC-induced apoptosis. Therefore, we examined the effect of expression of a constitutively active Myc-tagged form of AKT (myr-AKT) (27) on the activation of caspase-3 by 25-OHC treatment. We isolated a clone (clone B) stably expressing transfected myr-AKT (Fig. 3*A*). AKT activity in clone B cells was shown to be elevated ~2-fold relative to that in wild-type P388D1 cells as demonstrated *in vitro* by enzyme assay both in untreated and 25-OHC-treated cells (Fig. 3*B*). Clone B was also seen to be relatively resistant to induction of apoptosis by 25-OHC or 7-ketocholesterol as measured by caspase-3 activity (Fig. 3, *B* and *C*). To guard against the possibility that this result was due to another genetic variation in clone B, the ability of myr-AKT to protect cells from oxysterol-induced caspase-3 activation was also demonstrated by transient transfection with the same construct (Fig. 3*D*).

Effect of 25-OHC Treatment on BH3 Domain-only Proteins: Activation of BAD and Increased Cellular Levels of BIM—A common mechanism by which AKT inactivation is coupled to apoptosis is through the regulation of BAD by AKT (25). AKT phosphorylates BAD at two serine residues, resulting in its sequestration in the cytosol, bound to 14-3-3 (28–30). In the absence of ongoing AKT-catalyzed phosphorylation, BAD becomes dephosphorylated by any of several phosphatases (31). This results in its relocalization to the mitochondria (32–34),

where it heterodimerizes via its BH3 domain (35) with the anti-apoptotic BCL family members BCL-2 and BCL-x$_L$ (36). These are critical signaling events in the mitochondrial apoptotic pathway that result in canonical cytochrome *c* release (37). Because we have previously demonstrated that oxysterols mediate cytochrome *c* release from mitochondria during apoptotic induction in other cell types (19), we anticipated that a consequence of the observed AKT degradation would be activation of BAD.

BAD activation can be detected either through determination of its dephosphorylation or by its relocalization. We examined both processes. The immunoblot of BAD from 25-OHC-treated P388D1 cells with anti-phospho-BAD antibody is consistent with loss of phosphorylation (Fig. 4). In clone B, BAD was observed to be hyperphosphorylated both in untreated and 25-OHC-treated cells (Fig. 4), demonstrating the activity and, in particular, the anti-apoptotic activity of the myr-AKT construct in whole cells. The immunoblots of total mitochondrial BAD were consistent with an increase in the mitochondrial levels of BAD after 25-OHC treatment (data not shown). Relocalization of BAD was also demonstrated by transfection of murine RAW 264.7 macrophages with a BAD-GFP fusion protein. Such a reporter has previously been utilized to demonstrate BAD activation in another system (33). RAW 264.7 cells were used for this experiment because they grow attached and spread out on the surface of a plastic Petri dish, allowing better resolution of the cellular distribution of the
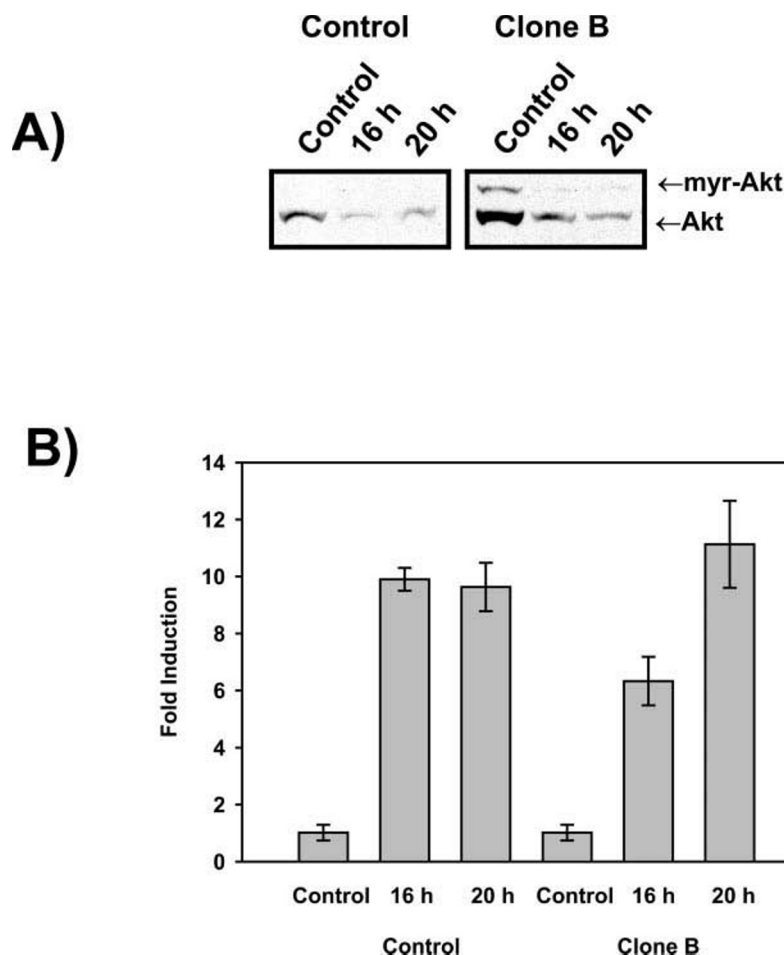
FIG. 8. **Caspase-3 activation after degradation of constitutively active myr-AKT in clone B P388D1 cells following prolonged treatment with 25-OHC.** *A*, immunoblot analysis of total AKT in whole cell lysates prepared from clone B and control P388D1 cells. Cells were incubated with or without 10 μg/ml 25-OHC for 16 and 20 h as indicated. *B*, caspase-3 activity was assayed in cells treated in parallel with those used for the AKT immunoblot shown in *A*.

fluorescent fusion protein. The results indicate a redistribution of BAD from a diffuse cytosolic localization to a punctate distribution largely colocalized with the mitochondrial marker MitoTracker (Fig. 5). This is precisely the result to be expected for the relocalization of BAD associated with dephosphorylation (33).

Korsmeyer and co-workers (38) have presented evidence for two classes of BH3 domain-only proteins. The first category is exemplified by BAD, which functions through "sensitization" toward apoptosis by heterodimerization and inactivation of anti-apoptotic multi-BCL homology domain family members. BH3 domain-only proteins in the second category activate the pro-apoptotic multi-BCL homology domain family members by inducing their oligomerization to release cytochrome *c*. Expression of one of these proteins (BIM) has been shown to be down-regulated by AKT (39). We therefore examined P388D1 cells for increased expression of BIM after 25-OHC treatment by immunoblotting. The results are consistent with an increase in BIM levels in cells and in mitochondria (Fig. 6).

Role of Multi-BCL Homology Domain Proteins in Induction of Apoptosis by 25-OHC—Release of cytochrome *c* from mitochondria in response to signaling by the BH3 domain-only proteins would be expected to involve two downstream events: the inactivation (sensitization) of the anti-apoptotic multi-BCL homology domain proteins and the activation of the pro-apoptotic multi-BCL homology domain proteins. As mentioned above, the potential targets of BAD are BCL-2 and BCL-xL. However, it has been reported that BAD can reverse the death repressor activity of only BCL-xL (36). Furthermore, immunoblot analysis indicated that P388D1 cells did not express BCL-2 (data not shown). This suggests that the target of BAD during 25-OHC induction of apoptosis is BCL-xL. It has been reported

that AKT up-regulates the expression of BCL-xL, suggesting the possibility that 25-OHC treatment might down-regulate its expression (39). Immunoblots of BCL-xL after 25-OHC treatment demonstrated that this did occur (Fig. 7*A*). Down-regulation of BCL-xL mRNA levels by 25-OHC as determined from Northern blots was also observed (data not shown).

As described above, the current thinking (38, 40) on the mechanism of BAD signaling in mitochondria is that BAD binding to BCL-xL would in turn activate the pro-apoptotic multi-BCL homology domain family members BAX and BAK to release cytochrome *c* (36, 41). Immunoblot analysis demonstrated that P388D1 cells expressed both BAK and BAX, with BAX having the usual (41) dual cytoplasmic and mitochondrial localization and BAK being found only in mitochondria (data not shown). It has been shown that BAX and BAK have overlapping functionality, but that suppression of BAX attenuates the apoptotic response to a variety of stimuli that act through the intrinsic pathway (42). To confirm that the BAX/BAK pathway operates as expected in the induction of apoptosis by oxysterols, we examined the effect of small interfering RNA knockdown of BAX on the apoptotic response to 25-OHC. After selection (see "Experimental Procedures"), we were able to isolate a clone of P388D1 cells (clone 1) that appeared to be highly reduced in BAX expression as determined by immunoblotting (Fig. 7*B*). This clone also exhibited no detectable apoptotic response to 25-OHC (Fig. 7*C*).

In contrast, prolonged exposure of clone B to 25-OHC still resulted in cell death and caspase-3 activation (Fig. 8*A*). This is apparently due to eventual degradation of the overexpressed, constitutively active AKT, resulting in a significant decrease in its cellular levels as measured by immunoblotting (Fig. 8*B*). This result is also consistent with the expression of constitu-

tively active AKT being the cause of the oxysterol resistance in clone B rather than an artifact of clone selection.

DISCUSSION

The results presented in this study are consistent with the conclusion that an important regulatory event in the induction of apoptosis by oxysterols is accelerated degradation of AKT. The activity of AKT has most commonly been described to be regulated by phosphorylation (24). In one well characterized apoptotic signal transduction pathway, that induced by ceramide, activation of protein phosphatase-2A (leading to dephosphorylation of AKT) plays a critical role (43). However, there have been other reports of regulated AKT degradation playing a role in apoptotic signal transduction pathways. For example, H_2O_2-induced apoptosis is accompanied by degradation of AKT (44), as is the induction of apoptosis by the 15-deoxyprostaglandin J_2 (45), both probable examples of apoptosis with reactive oxygen species second messengers (44, 46). It is worth noting, in this context, that reactive oxygen species have been suggested to play a role in oxysterol-induced apoptosis (14, 20).

An important consideration is whether the activation of AKT degradation is upstream or downstream of the many caspases activated during apoptosis. Our data are consistent with activation of AKT degradation being an early event. First, the degradative response was observed in as little as 30 min after 25-OHC addition (Fig. 2C), whereas we have previously observed caspase-3 activation to be undetectable in response to 25-OHC treatment in as much as 5 h (19). Second, the inhibition of degradation by a proteasome inhibitor (Fig. 2D) is consistent with a non-caspase-mediated degradatory process. Finally and most tellingly, overexpression of a constitutively active AKT (myr-AKT) in clone B delayed the activation of caspase-3 by 25-OHC, consistent with caspase activation being downstream of AKT degradation rather than the other way around. It is also noteworthy that the eventual degradation of myr-AKT produced by 25-OHC treatment can still result in capsase-3 activation, consistent with a temporal pattern of AKT degradation preceding caspase-3 activation.

The responses of the various BCL family members studied in this work are predictable from the loss of AKT activity. The role of AKT in phosphorylation and inactivation of BAD is well documented (25, 28–36); and therefore, it is not surprising that loss of AKT resulted in dephosphorylation of BAD (Fig. 4) and its relocalization to the mitochondria (Figs. 4 and 5), where it would be expected to heterodimerize with the anti-apoptotic multi-BCL homology domain family members. Further sensitization to apoptotic induction is achieved through loss of AKT because of its role in signaling transcriptional up-regulation, through the NF-κB pathway (47–49), of the anti-apoptotic multi-BCL homology domain family member BCL-x_L (39, 50).

Transcriptional down-regulation of the BH3 domain-only protein BIM by AKT has also been reported (39), and our observation of increased BIM expression in whole cells and mitochondria (Fig. 6) in response to 25-OHC is consistent with this prior work. In the mitochondrial apoptotic pathway, BIM functions to stimulate the oligomerization of the pro-apoptotic multi-BCL homology domain family members BAX and BAK, thereby producing the release of cytochrome c (38).

Sensitization to apoptotic induction by down-regulation of BCL-x_L and relocalization of BAD to mitochondria and expression of BIM should lead to activation of BAX/BAK. Somewhat surprisingly, rather than attenuation of apoptosis in response to 25-OHC treatment after small interfering RNA knockdown of BAX, we were able to isolate, by immunoblotting, a clone with no detectable BAX that exhibited no detectable apoptotic response (Fig. 8). It has been reported that some stimuli, no-

tably staurosporine, that operate through the intrinsic apoptotic pathway are more responsive to BAX knockout than to BAK knockout (42), and we may have observed such a differential response to 25-OHC.

It has been reported that another oxysterol, 7-ketocholesterol, activates apoptosis in fibroblasts through a signal transduction pathway that requires phosphorylation of STAT1 at Ser-727 (51). This is noteworthy because some signal transduction pathways to STAT1 serine phosphorylation proceed through AKT (52). However, reports have appeared that have implicated other kinases in STAT1 serine phosphorylation, including p38 mitogen-activated protein kinase and protein kinase C(53, 54). Ser-727 phosphorylation in macrophages, in particular, seems to be more dependent on these other kinases (54).

While this manuscript was under review, a report appeared describing the Ca^{2+} release-mediated activation of the endoplasmic reticulum unfolded protein response pathway during the induction of apoptosis by free cholesterol loading of macrophages (23). The endoplasmic reticulum was interpreted to be the site of cholesterol damage leading to the calcium signal. The oxysterol induction of apoptosis appears to be different, at least in some respects, from this system because oxysterol apoptotic signaling appears to proceed through a signal transduction pathway requiring arachidonic acid release (9) and possibly reactive oxygen species formation (14, 20), both of which might be expected to be upstream of the AKT degradation reported here. Whether cholesterol loading can activate AKT degradation and whether oxysterols can activate one or more elements of the unfolded protein response remain to be determined.

REFERENCES

1. Witztum, J. L., and Steinberg, D. (2001) *Trends Cardiovasc. Med.* **11,** 93–102
2. Steinbrecher, U. P. (1999) *Biochim. Biophys. Acta* **1436,** 279–298
3. Hardwick, S. J., Hegyi, L., Clare, K., Law, N. S., Carpenter, K. L., Mitchinson, M. J., and Skepper, J. N. (1996) *J. Pathol.* **179,** 294–302
4. Wintergerst, E. S., Jelk, J., Rahner, C., and Asmis, R. (2000) *Eur. J. Biochem.* **267,** 6050–6059
5. Rusiñol, A. E., Yang, L., Thewke, D., Panini, S. R., Kramer, M. F., and Sinensky, M. S. (2000) *J. Biol. Chem.* **275,** 7296–7303
6. Martinet, W., and Kockx, M. M. (2001) *Curr. Opin. Lipidol.* **12,** 535–541
7. Colles, S. M., Maxson, J. M., Carlson, S. G., and Chisholm, G. M. (2001) *Trends Cardiovasc. Med.* **11,** 131–138
8. Muller, K., Dulku, S., Hardwick, S. J., Skepper, J. N., and Mitchinson, M. J. (2001) *Atherosclerosis* **156,** 133–144
9. Panini, S. R., Yang, L., Rusiñol, A. E., Sinensky, M. S., Bonventre, J. V., and Leslie, C. C. (2001) *J. Lipid Res.* **42,** 1678–1686
10. Schroepfer, G. J. (2000) *Physiol. Rev.* **80,** 361–554
11. Chisolm, G. M., Ma, G., Irwin, K. C., Martin, L. L., Gunderson, K. G., Linberg, L. F., Morel, D. W., and DiCorleto, P. E. (1994) *Proc. Natl. Acad. Sci. U. S. A.* **91,** 11452–11456
12. Sevanian, A., Hodis, H. N., Hwang, J., McLeod, L. L., and Peterson, H. (1995) *J. Lipid Res.* **36,** 1971–1986
13. Panini, S. R., and Sinensky, M. S. (2001) *Curr. Opin. Lipidol.* **12,** 529–533
14. Harada-Shiba, M., Kinoshita, M., Kamido, H., and Shimokado, K. (1998) *J. Biol. Chem.* **273,** 9681–9687
15. Aupeix, K., Weltin, D., Mejia, J. E., Christ, M., Marchal, J., Freyssinet, J.-M., and Bischoff, P. (1995) *Immunobiology* **194,** 415–428
16. Harada, K., Ishibashi, S., Miyashita, T., Osuga, J.-I., Yagyu, H., Ohashi, K., Yazaki, Y., and Yamada, N. (1997) *FEBS Lett.* **411,** 63–66
17. Bansal, N., Houle, A., and Melnykovych, G. (1991) *FASEB J.* **5,** 211–216
18. Christ, M., Luu, B., Mejia, J. E., Moosbrugger, I., and Bischoff, P. (1993) *Immunology* **78,** 455–460
19. Yang, L., and Sinensky, M. S. (2000) *Biochem. Biophys. Res. Commun.* **278,** 557–563
20. Lizard, G., Gueldry, S., Sordet, O., Monier, S., Athias, A., Miguet, C., Bessede, G., Lemaire, S., Solary, E., and Gambert, P. (1998) *FASEB J.* **12,** 1651–1663
21. Kaufmann, S. H., and Hengartner, M. O. (2001) *Trends Cell Biol.* **11,** 526–534
22. Shinohara, H., Balboa, M. A., Johnson, C. A, Balsinde, J., and Dennis, E. A. (1999) *J. Biol. Chem.* **274,** 12263–12268
23. Feng, B., Yao, P. M., Li, Y., Devlin, C. M., Zhang, D., Harding, H. P., Sweeney, M., Rong, J. X., Kuriakose, G., Fisher, E. A., Marks, A. R., Ron, D., and Tabas, I. (2003) *Nat. Cell Biol.* **5,** 781–792
24. Downward, J. (1998) *Curr. Opin. Cell Biol.* **10,** 262–267
25. Nunez, G., and del Peso, L. (1998) *Curr. Opin. Neurobiol.* **8,** 613–618

26. Liu, H., Perlman, H., Pagliari, L. J., and Pope, R. M. (2001) *J. Exp. Med.* **194,** 113–126
27. Kohn, A. D., Summers, S. A., Birnbaum, M. J., and Roth, R. A. (1996) *J. Biol. Chem.* **271,** 31372–31378
28. Zha, J., Harada, H., Yang, E., Jockel, J., and Korsmeyer, S. J. (1996) *Cell* **87,** 619–628
29. del Peso, L., Gonzalez-Garcia, M., Page, C., Herrera, R., and Nunez, G. (1997) *Science* **278,** 687–689
30. Datta, S. R., Dudek, H., Tao, X., Masters, S., Fu, H., Gotoh, Y., and Greenberg, M. E. (1997) *Cell* **91,** 231–241
31. Klumpp, S., and Krieglstein, J. (2002) *Curr. Opin. Pharmacol.* **2,** 458–462
32. Pastorino, J. G., Tafani, M., and Farber, J. L. (1999) *J. Biol. Chem.* **274,** 19411–19416
33. Wang, H.-G., Pathan, N., Ethell, I. M., Krajewski, S., Yamaguchi, Y., Shibasaki, F., McKeon, F., Bobo, T., Franke, T. F., and Reed, J. C. (1999) *Science* **284,** 339–343
34. Cheng, E. H., Wei, M. C., Weiler, S., Flavell, R. A., Mak, T. W., Lindsten, T., and Korsmeyer, S. J. (2001) *Mol. Cell* **8,** 705–711
35. Zha, J., Harada, H., Osipov, K., Jockel, J., Waksman, G., and Korsmeyer, S. J. (1997) *J. Biol. Chem.* **272,** 24101–24104
36. Yang, G., Zha, J., Jockel, J., Boise, L. H., Thompson, C. B., and Korsmeyer, S. J. (1995) *Cell* **80,** 285–291
37. Wang, X. (2001) *Genes Dev.* **15,** 2922–2933
38. Letai, A., Bassik, M. C., Walensky, L. D., Sorcinelli, M. D., Weiler, S., and Korsmeyer, S. J. (2002) *Cancer Cell* **2,** 183–192
39. Dijkers, P. F., Birkenkamp, K. U., Lam, E. W., Thomas, N. S., Lammers, J. W., Koenderman, L., and Coffer, P. J. (2002) *J. Cell Biol.* **156,** 531–542
40. Moreau, C., Cartron, P. F., Hunt, A., Meflah, K., Green, D. R., Evan, G., Vallette, F. M., and Juin, P. (2003) *J. Biol. Chem.* **278,** 19426–19435
41. Scorrano, L., and Korsmeyer, S. J. (2003) *Biochem. Biophys. Res. Commun.* **304,** 437–444
42. Wei, M. C., Zong, W. X., Cheng, E. H., Lindsten, T., Panoutsakopoulou, V., Ross, A. J., Roth, K. A., MacGregor, G. R., Thompson, C. B., and Korsmeyer, S. J. (2001) *Science* **292,** 727–730
43. Ruvolo, P. (2003) *Pharmacol. Res.* **47,** 387–392
44. Martin, D., Salinas, M., Fujita, N., Tsuruo, T., and Cuadrado, A. (2002) *J. Biol. Chem.* **277,** 42943–42952
45. Rovin, B. H., Wilmer, W. A., Lu, L., Doseff, A. L., Dixon, C., Kotur, M., and Hilbelink, T. (2002) *Kidney Int.* **61,** 1293–1302
46. Hortelano, S., Castrillo, A., Alvarez, A. M., and Bosca, L. (2000) *J. Immunol.* **165,** 6525–6531
47. Ozes, O. N., Mayo, L. D., Gustin, J. A., Pfeffer, S. R., Pfeffer, L. M., and Donner, D. B. (1999) *Nature* **401,** 82–85
48. Glasgow, J. N., Qiu, J., Rassin, D., Grafe, M., Wood, T., and Perez-Pol, J. R. (2001) *Neurochem. Res.* **26,** 647–659
49. Mori, N., Yamada, Y., Ikeda, S., Yamasaki, Y., Tsukasaki, K., Tanaka, Y., Tomonaga, M., Yamamoto, N., and Fujii, M. (2002) *Blood* **100,** 1828–1834
50. Kirito, K., Watanabe, T., Sawada, K., Endo, H., Ozawa, K., and Komatsu, N. (2002) *J. Biol. Chem.* **277,** 8329–8337
51. Agrawal, S., Agrawal, M. L., Chatterjee-Kishore, M., Stark, G. R., and Chisolm, G. M. (2002) *Mol. Cell. Biol.* **22,** 1981–1992
52. Nguyen, H., Ramana, C. V., Bayes, J., and Stark, G. R. (2001) *J. Biol. Chem.* **276,** 33361–33368
53. Song, J. H., So, E. Y., and Lee, C. E. (2002) *Mol. Cells* **13,** 322–326
54. Rhee, S. H., Jones, B. W., Toshchakov, V., Vogel, S. N., and Fenton, M. J. (2003) *J. Biol. Chem.* **278,** 22506–22512